Towards Fully Nonempirical Simulations of Optical Band Shapes Of Molecules in Solution: A Case Study of Heterocyclic Ketoimine Difluoroborates

ARTICLE *in* THE JOURNAL OF PHYSICAL CHEMISTRY A · MAY 2015

Impact Factor: 2.69 · DOI: 10.1021/jp5094417

7 AUTHORS, INCLUDING:

Natarajan Arul Murugan
KTH Royal Institute of Technology
72 PUBLICATIONS **574** CITATIONS
SEE PROFILE

Borys Osmialowski
UTP University of Science and Technology
130 PUBLICATIONS **968** CITATIONS
SEE PROFILE

Wojciech Bartkowiak
Wroclaw University of Technology
111 PUBLICATIONS **1,264** CITATIONS
SEE PROFILE

Hans Agren
KTH Royal Institute of Technology
867 PUBLICATIONS **18,728** CITATIONS
SEE PROFILE

THE JOURNAL OF PHYSICAL CHEMISTRY A

Article

pubs.acs.org/JPCA

Toward Fully Nonempirical Simulations of Optical Band Shapes of Molecules in Solution: A Case Study of Heterocyclic Ketoimine Difluoroborates

Robert Zaleśny,*[,†] N. Arul Murugan,[†] Faris Gel'mukhanov,[†] Zilvinas Rinkevicius,[†,‡] Borys Ośmiałowski,[§] Wojciech Bartkowiak,[∥] and Hans Ågren*[,†]

[†]Division of Theoretical Chemistry and Biology, School of Biotechnology and [‡]Swedish e-Science Research Center, Royal Institute of Technology, SE-10691 Stockholm, Sweden

[§]Faculty of Chemical Technology and Engineering, UTP University of Science and Technology, Seminaryjna 3, PL-85326 Bydgoszcz, Poland

[∥]Institute of Physical and Theoretical Chemistry, Wroclaw University of Technology, Wyb. Wyspiańskiego 27, PL-50370 Wrocław, Poland

Supporting Information

ABSTRACT: This study demonstrates that a hybrid density functional theory/molecular mechanics approach can be successfully combined with time-dependent wavepacket approach to predict the shape of optical bands for molecules in solutions, including vibrational fine structure. A key step in this treatment is the estimation of the inhomogeneous broadening based on the hybrid approach, where the polarization between solute and atomically decomposed solvent is taken into account in a self-consistent manner. The potential of this approach is shown by predicting optical absorption bands for three heterocyclic ketoimine difluoroborates in solution.

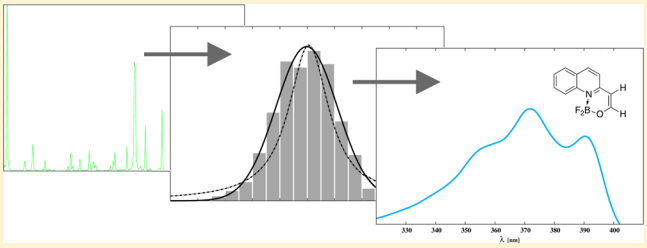

INTRODUCTION

First-principles prediction of electronic absorption and emission spectra of molecules lies at the heart of computational quantum chemistry. Tremendous efforts are still made to develop and benchmark efficient approaches to determine electronic structure and properties of molecules. Among them, the time-dependent density functional theory (TD-DFT) has recently gained in popularity due to its computational efficiency. Despite some well-recognized drawbacks of exchange−correlation functionals, like for instance failures in description of charge-transfer or Rydberg states,[1] TD-DFT is nowadays the most widely applied approach to determine electronic spectra of medium- and large-sized molecules.[2,3] Recent exhaustive studies by Jacquemin's group indicate that, on average, the predictive power of TD-DFT is comparable to the power of some popular wave function-based methods, like for instance the coupled-cluster CC2 model.[4−7] As recently demonstrated by Jacquemin et al.,[8] and also by other authors,[9−11] one of the possibilities to improve predictions of vertical and 0−0 excitation energies computed using TD-DFT is to tune range-separated hybrid functionals. A majority of applications of TD-DFT in studies of electronic structure of medium- and large-sized molecules falls into the "vertical energy" (VE) or the so-called crude adiabatic approximation rubric; i.e., the excitation energy is computed at the ground state molecular geometry and the effect of nuclear motion is neglected. As pointed out by Lasorne et al.,[12] the VE approximation might introduce an error larger than 0.1 eV in comparison to absorption maxima, something that makes the assessment of theoretical methods more difficult. Thus, an explicit treatment of nuclear motion is mandatory to refine the computational protocol and yet to allow for simulations of fine structure of optical band shapes. In fact, there is rapid progress in this field.[13−17] Efficient algorithms have been developed in the form of computer codes to determine Franck−Condon (FC) factors and Herzberg−Teller (HT) contributions, even including mechanical anharmonicity. Moreover, there are some implementations within the spirit of time-dependent wavepacket theory by Heller and co-workers[18] that offer some advantages over conventional evaluation of matrix elements. As shown recently by Silverstein and Jensen, the wavepacket simulations can also be successfully applied in the domain of multiphoton spectroscopy.[14,15,19] Because a scaling of TD-DFT with respect to the number of basis functions in the Kohn−Sham framework is relatively low, it comes as little suprise that this method is the most common choice for simulations of

Special Issue: Jacopo Tomasi Festschrift

Received: September 17, 2014
Revised: November 21, 2014
Published: November 22, 2014

vibrational fine structure of optical bands in electronic spectroscopy.[4,20−29]

Due to the fact that electronic absorption and emission spectra of molecules are usually recorded in condensed phases, the effect of environment also needs to be included in the computational protocol to reliably predict properties in question using first-principles simulations. It is fair to mention that there are already routes to simulate optical band shapes including both the effect of vibrational motions and solvent influence, which is also central to the present study. As recently highlighted by De Mitri et al.,[30] the choice of the computational protocol to simulate optical band shape and its complex features depends to a large extent on the conformational flexibility of the dye. Basically, the approaches to predict the complex features of absorption bands in optical spectra fall into two categories.

The first category, best suited for flexible dyes, is sometimes referred to as the time-dependent statistical approach and combines classical sampling combined with a quantum-mechanical description of electronic structure of a dye in solution (see, for instance, refs 30−37 and references therein). Recent and very successful application of this approach was reported by Barone's group to predict the absorption and emission spectra of flexible dye (4-(naphthoyloxy)-1-methoxy-2,2,6,6-tetramethylpiperidine) in solution.[30] These authors performed atomistic simulations using accurately parametrized force fields and the transition energies computed using TD-DFT on a set of snapshots from MD simulations were convoluted with the Gaussian function to yield the final band shape (half-width at half-maximum (HWHM) was set to 0.05 eV for each snapshot). Note that some authors determine the spectral width on the basis of the distribution of vertical excitation energies.[35] Some interesting insight into this subject has recently been presented by Eilmes.[38]

The second category, more suitable for less flexible dyes, relies on calculations performed in a time-independent fashion. The geometry of a solute is optimized in the presence of a solvent (polarizable continuum solvation model (PCM) is a common choice[39,40]), and the electronic and vibrational structure calculations are performed using quantum chemistry methods. This allows us to determine stick FC and/or FC-HT and HT spectra corresponding to transitions between vibrational levels in the ground and excited states, with solvent effects included in the treatment. To determine the absorption (emission) band shape, it is common to assign some arbitrary broadening to each individual stick transition so that the experimental optical band can be reproduced (multiphoton spectra can be determined in a likewise manner[41]).

It should be highlighted that the predictive power of the two above outlined routes to simulation of complex features of optical band shapes crucially depends on the magnitude of the parameters corresponding to spectral broadening. In the case of substantial environmental broadening, the vibrational fine structure is expected to be completely washed out and any successful computational protocol is expected to predict such an effect. Recently, Ferrer et al. have demonstrated, on the basis of a basic relationship between the reorganization energy and the inhomogeneous broadening and with the results of the recently developed state specific implementation of PCM-TDDFT, that it is possible to successfully estimate the polar contribution to the inhomogeneous broadening.[42] These authors determined fully nonempirical absorption spectra of coumarin C153 in three solvents, obtaining spectral widths in excellent agreement with the experimental data. As highlighted recently by Ferrer et al., several effects are not expected to be reliably treated by PCM and thus there is still need for studies combining explicit and implicit solvation to reliably predict the inhomogeneous broadening.[43] The present study is a step in this direction and makes an attempt to combine implicit and explicit solvation to predict fully *ab initio* optical absorption band shapes, including vibrational fine structure. In so doing, we determine the FC spectrum using the time-dependent wavepacket approach, simultaneously taking into account the environmental broadening estimated at the density functional self-consistent quantum mechanics/molecular mechanics theory. Three newly synthesized heterocyclic ketoimine difluoroborates (cf. Figure 1) were chosen to demonstrate the predictive power of the method as they exhibit vibrational fine structure of absorption and emission bands in many solvents.

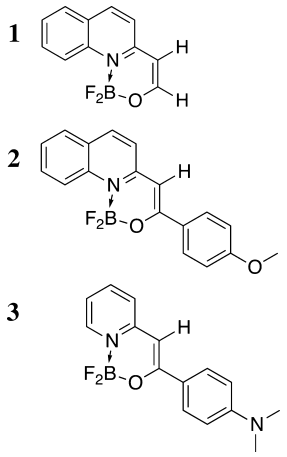

Figure 1. Heterocyclic ketoimine difluoroborates studied in the present work.

THEORY AND COMPUTATIONAL DETAILS

The computational protocol employed in the present study to simulate absorption band shapes involves several steps, and they are shown in the flowchart presented in Figure 2. In what follows we outline computational details corresponding to each step.

Electronic and Vibrational Structure Calculations. The geometries of all studied molecules in their electronic ground state were optimized at the CAM-B3LYP/6-311++G(d,p) level of theory.[44] At the very same level of theory we computed the ground state Hessian and the energy gradient in the first singlet excited state. On the basis of these quantities, we determined the dimensionless normal mode displacements between the first excited state and the ground state. The choice of the CAM-B3LYP exchange−correlation functional for this study stems from recent reports that excited state gradients are predicted more accurately in comparison to other functionals.[45] Unless otherwise indicated, the solvent influence was included in these calculations by employing the LR-PCM[46,47] using the GAUSSIAN 09 suite of programs.[48] Moreover, for one molecule (**1**) we also performed electronic and vibrational structure calculations *in vacuo*, at the CC2/cc-pVTZ level of theory.[49] In that event we used the TURBOMOLE program.[50]

Molecular Dynamics Simulations. The optical properties of heterocyclic ketoimine difluoroborates were studied in two

dx.doi.org/10.1021/jp5094417 | J. Phys. Chem. A 2015, 119, 5145−5152

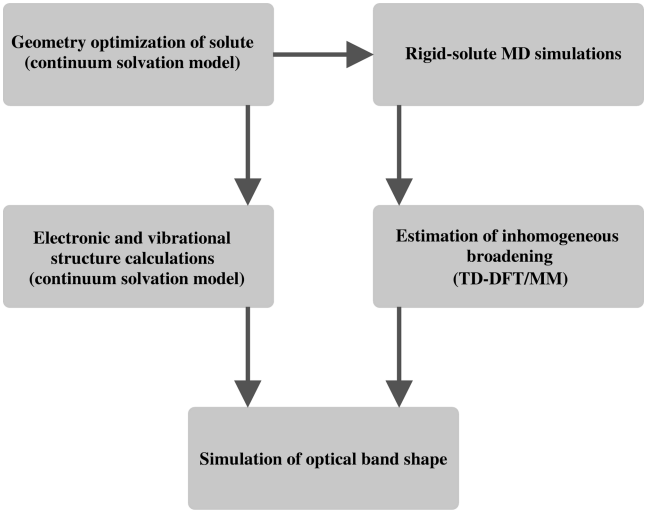

Figure 2. Schematic representation of the computational protocol.

different solvents, namely chloroform (molecules **1** and **2**) and dimethylformamide (hereafter referred to as DMF; molecule **3**). In all simulations reported herein, a rigid molecular model was employed for the solute; that is, the geometry of each system was kept frozen in its optimized conformation in the respective solvent. The geometries were obtained at the B3LYP/6-311++G(d,p) level of theory using the polarizable continuum solvation model. The interaction parameters for boron were taken from the work of Amirjalayer et al.[51] whereas the equilibrium bond length and bond angle values involving the boron atom correspond to the optimized geometries. Chloroform and dimethylformamide solvent molecules were added to prepare two sets of solute−solvent input structures that were used in the molecular dynamics simulations. The number of chloroform and DMF molecules added were respectively 2240 (solvation of **1** and **2**) and 1430 (solvation of **3**). As we mentioned earlier, we use a rigid molecular model for solutes whereas the solvent molecules are fully flexible. The generalized AMBER force-field[52] is employed to describe all subsystems. The charges for solute molecules in the respective solvents were derived using the CHELPG[53] procedure as implemented in GAUSSIAN 09 package.[48] The same procedure was used to derive the charges for chloroform and DMF solvent. The simulations were carried out, using the AMBER 11 software,[54] in isothermal−isobaric ensemble to allow solute−solvent systems to reach the appropriate density. The external thermodynamic variables for the simulations were kept at 1 atm pressure and 300 K, which have been achieved by connecting the solute−solvent system to the Nosé thermostat and barostat, respectively. The time scale for integrating the equation of motion was chosen as 1 fs. Equilibration runs were carried out until the solute−solvent systems attained converged density. The productions runs were carried out for 10 ns (**2**, **3**) and 50 ns (**1**).

TD-DFT/MM. An essential step of the computational treatment employed in the present study is the estimation of the spectral broadening due to the environment. This is achieved by employing a hybrid density functional theory/molecular mechanics approach (hereafter referred to as TD-DFT/MM), which retains a discrete representation of the solvent environment. In this method, the polarization between the solute and solvent is taken into account using a self-consistent scheme, linear in the solvent polarization.[55,56] In the case of **1**, 1000 solute−solvent configurations from rigid-body molecular dynamics simulations were selected at equal intervals from the trajectory corresponding to 50 ns and used in TD-DFT/MM calculations. In the case of **2** and **3**, 100 configurations were picked up for each conformation from the 10 ns trajectory (see next section for details). For a set of solute−solvent configurations, the TD-DFT/MM calculations of excitation energies were performed using linear response functions at the CAM-B3LYP/TZVP level of theory. The polarizable force fields in TD-DFT/MM method were derived on the basis of the LoProp approach[57] for both solvents (i.e., chloroform and DMF). A cutoff equal to 15 Å (from a solute center of mass) was assumed to define solvation box in TD-DFT/MM calculations so that 102, 99, and 114 solvent molecules were included in the case of **1**, **2** and **3**. TD-DFT/MM computations were performed using the DALTON program.[58]

Time-Dependent Wavepacket Calculations. To simulate the vibrational structure of absorption band, we have employed the time-dependent wavepacket approach pioneered by Heller and co-workers.[18] The one-photon absorption cross section (σ) was determined assuming Born−Oppenheimer and Franck−Condon approximations and is given by[59]

$$\sigma(E_L) = \frac{4\pi}{3\hbar c} E_L \sum_n (M_{0n})^2 \operatorname{Re} \int_0^\infty \langle i|i_n(t)\rangle e^{i(E_L - E_{0n} + \varepsilon_{i0} + i\Gamma_n)t}\, dt \quad (1)$$

where E_L stands for the energy of incident photon, n denotes the electronic state. ε_i stands for the energy of vibrational state $|i\rangle$; Γ_n and M_{0n} correspond to the homogeneous line width and electric transition dipole moment between the ground state 0 and state n, respectively. $|i_n(t)\rangle$ is a wave packet in nth excited state. The one-photon cross section (σ) was determined employing the independent mode displaced harmonic oscillator (IMDHO) model. All wavepacket simulations were performed with either custom software or the aid of the *orca_asa* program, which is a part of the ORCA package.[60] Details of implementation in ORCA package can be found elsewhere.[59]

RESULTS AND DISCUSSION

The molecules presented in Figure 2 constitute the test set for the protocol outlined in the previous section. These newly synthesized heterocyclic ketoimine difluoroborates (see Supporting Information for details regarding synthesis of these compounds), similarly to other BODIPY derivatives, exhibit vibrational fine structure of absorption and emission bands in many solvents.[61] Compound **1** shows clear vibrational structure of the absorption band in chloroform solution (cf. Figure 4). Either the other two molecules show vibrational structure only weakly (molecule **2** in chloroform solution, cf. Figure 5) or the vibrational structure is completely washed out (molecule **3** in DMF solution, cf. Figure 6). The interest in the molecules carrying BF_2 moiety, similarly to BODIPY and related families of compounds, is largely due to their fluorescent properties; i.e., they exhibit quite significant values of fluorescence quantum yield, thus showing a potential for many applications, including ion pair recognition,[62] photovoltaic devices,[63] pH[64] (and CO_2[65]) probes, and bioimaging in living cells.[66] The BODIPY dyes are characterized, however, by small Stokes shifts, yielding overlapped absorption and emission spectra. Thus, there is a need to find new ways to obtain this kind of molecule with

dx.doi.org/10.1021/jp5094417 | J. Phys. Chem. A 2015, 119, 5145−5152

tunable photophysical properties. This area is rapidly growing and we kindly refer to a recent review on BF_2-carrying compounds.[61] In what follows, we will present the results of calculations for each system.

We will start with the analysis of the estimation of environmental broadening for molecule **1**. As already mentioned in the preceding section, we performed molecular dynamic simulations, treating molecule **1** as completely rigid while the chloroform molecules were allowed to change their positions around the solute. A total of 1000 solute/solvent configurations was selected for TD-DFT/MM calculations of electronic structure. The instantaneous positions of solvent molecules around solute give rise to distribution of 0−0 excitation energies. In this study, instead, we make an approximation and analyze the distribution of the vertical excitation energies to a final state n (E^v_{0n}) around an average value ($\bar{E}^v_{0n}$). The histogram showing the number of snaphots per vertical excitation energy interval (0.01 eV) for molecule **1** is given in Figure 3. The histogram normalized to unity was

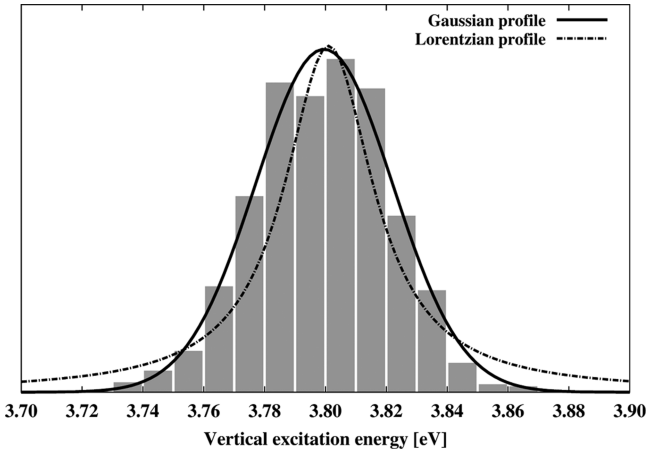

Figure 3. Normalized histogram of vertical excitation energies for **1** in chloroform. The data were obtained at the CAM-B3LYP/TZVP level of theory and correspond to 1000 solute−solvent configurations.

fitted using the Levenberg−Marquardt algorithm by two line profiles, namely normalized Lorentzian function:

$$l(E^v_{0n}) = \frac{1}{\pi}\frac{\Gamma_{0n}}{(E^v_{0n} - \bar{E}^v_{0n})^2 + (\Gamma_{0n})^2} \quad (2)$$

and normalized Gaussian function:

$$g(E^v_{0n}) = \frac{1}{\Theta_n\sqrt{2\pi}}\exp\left[-\frac{1}{2}\left(\frac{E^v_{0n} - \bar{E}^v_{0n}}{\Theta_n}\right)^2\right] \quad (3)$$

where Θ_n is the standard deviation corresponding to Gaussian distribution of excitation energies E^v_{0n} (note that hereafter Γ stands for half-width at half-maximum (HWHM) and in the case of Gaussian distribution $\Gamma = \Theta(2\ln 2)^{1/2}$). As seen in Figure 3, the Gaussian function is a better choice to describe the environmental broadening (Γ_{INH}). The value of standard deviation estimated on the basis of the histogram fitting was found to be Θ = 170 cm^{-1} (corresponding HWHM (Γ_{INH}) is 200 cm^{-1}), whereas the value computed as the square root of the variance for 1000 snapshots is 177 cm^{-1}. It is worthwile highlighting that the value of standard deviation computed for 100 snapshots is only 5% larger than that determined for 1000 snapshots. This rather small value of standard deviation reflects a relatively neglibible influence of chloroform solution on the $\pi \rightarrow \pi^*$ transition for molecule **1**. We have also performed the calculations for 1000 configurations based on the force field where solvent molecules are represented solely by charges; the corresponding value of standard deviation is 173 cm^{-1}. There is an extensive literature on spectral broadening in liquids (we refer to an exhausting review by Myers[67] on this subject). In short, the Gaussian-like distribution of electronic energy gaps due to local environments of solutes is referred to as inhomogeneous broadening. On the basis of the thus calculated value of Γ_{INH}, we determined the total absorption cross section (σ_{tot}) as convolution of the Franck−Condon spectra (σ_{FC}) and the normalized Gaussian function (cf. eq 3) corresponding to the environmental broadening:

$$\sigma_{tot}(\omega) = \int \sigma_{FC}(\omega')\, g(\omega-\omega')\, d\omega' \quad (4)$$

Simulations of Franck−Condon spectra were performed on the basis of the complete set of normal modes in the case of molecule **1** and assuming homogeneous (Lorentzian) broadening Γ_H = 10 cm^{-1}. The results of simulations and comparison with experimental data are presented in Figure 4. Let us discuss

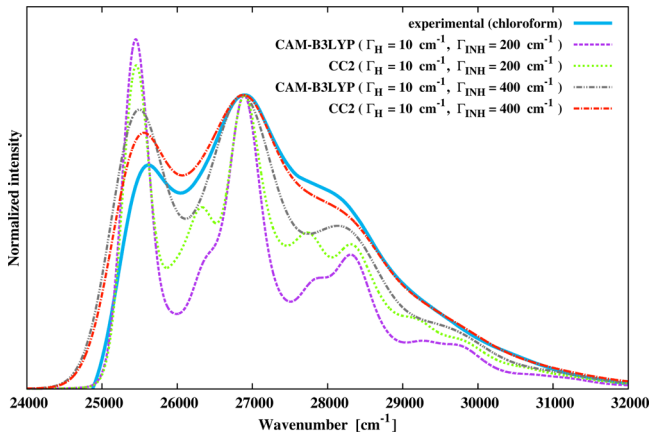

Figure 4. Experimental and simulated spectra of **1** in chloroform. In the case of CAM-B3LYP and CC2 calculations we used 6-311++G(d,p) and cc-pVTZ basis sets, respectively. Simulated spectra were shifted to match the experimental one.

first the results of simulations based on eq 4) with Γ_{INH} = 200 cm^{-1}. The plot demonstrates that the ratio of band shoulders is not reproduced satisfactorily on the basis of the simulations using the CAM-B3LYP functional (the assignments of the most intense features are presented in the Supporting Information). To shed more light on this subject, we have performed an additional set of calculations using the CC2 method and the cc-pVTZ basis set. Due to the computational cost connected with these calculations, we have performed CC2 calculations of frequencies, and dimensionless displacements (related to the Huang−Rhys factors) for the molecule *in vacuo*. The intensity ratio for band shoulders is better predicted by the CC2 method. This suggests that CAM-B3LYP has difficulty in predicting accurately the Huang−Rhys factors for this particular system. We have performed similar calculations using the B3LYP and PBE0 functionals (results are not shown) and their predictions were likewise. As shown by the results for molecule **1**, global hybrids do not seem to be the optimal choice for this particular molecule. As shown by Boulanger et al. for similar compounds,

dx.doi.org/10.1021/jp5094417 | J. Phys. Chem. A 2015, 119, 5145−5152

the use of the Bethe−Salpeter scheme might improve the predictions of absorption spectra.[68]

Figure 4 reveals that there is too much vibrational structure seen in the absorption band of **1**. To obtain better agreement with the experimental spectrum, we performed simulations based on eq 4, adjusting the value of the HWHM corresponding to a Gaussian profile. The best fit of simulated spectra with experiment is found for Γ_{INH}^{fit} = 400 cm^{-1}. The difference between Γ_{INH} estimated from the TD-DFT/MM approach and that found by fitting to experiment can be attributed not only to a deficiency of the computational protocol but also to a large extent to the instrumental broadening (spectral resolution of UV/vis spectrophotometer). Assuming that the difference can be considered as coming due to a Gaussian-like broadening, the corresponding value of Γ_{INH}^{Δ} is 346 cm^{-1} (note that $\Gamma_{INH}^{\Delta} = [(\Gamma_{INH}^{fit})^2 - \Gamma_{INH}^{2}]^{1/2}$.

Molecules **2** and **3** are much more flexible than **1** due to the presence of a phenyl ring attached to the heterocyclic moiety. This additional conformation flexibility is expected to contribute to the spectral width of corresponding absorption band. To account for this contribution, we treat the torsional mode classically; i.e., we have performed a series of rigid-body MD simulations freezing the interplanar angle between the phenyl ring and heterocyclic moiety. Each of 10 conformations used in the rigid-solute MD simulations, spanning a range from 0 to 180° with steps of 20°, was partially optimized at the B3LYP/6-311++G(d,p) level of theory. From each MD simulation we then extracted 100 solute−solvent configurations for TD-DFT/MM calculations. In total, on the basis of 1000 snapshots, we generated histogram of excitation energies (we used Boltzmann weighting according to total energy of a solute in solvent as computed at the TD-DFT/MM level) and the standard deviation was estimated. In the case of **2** the value of Θ was found to be 546 cm^{-1} (corresponding Γ_{INH} is equal to 643 cm^{-1}). The time-dependet wavepacket simulations were performed including all but the lowest-frequency normal mode corresponding to torsional vibration of phenyl ring. The results of the time-dependent wavepacket simulations for molecule **2** are presented in Figure 5. Similarly to the simulations for molecule **1**, we have performed wavepacket calculations for two values of HWHM, namely $\Gamma_{INH,1}$ = 643 cm^{-1} and $\Gamma_{INH,2}$ = 731 cm^{-1}. The latter value corresponds to the HWHM after convolution of two Gaussian profiles, i.e., $\Gamma_{INH,2} = g(\omega,\Gamma_{INH,1}) \otimes g(\omega,\Gamma_{INH}^{\Delta}) = [\Gamma_{INH,1}^{2} + (\Gamma_{INH}^{\Delta})^2]^{1/2}$. As seen from the plot, a slightly better agreement is found for the former value. It should be highlighted that the overall band shape is reproduced satisfactorily regardless of the value of Γ_{INH} used in the wavepacket simulations.

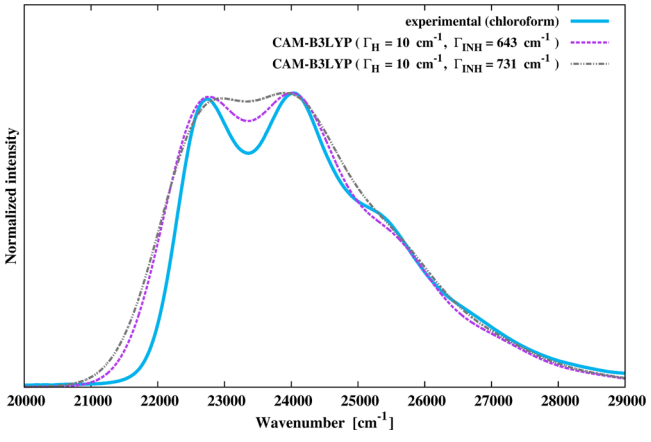

Figure 5. Experimental and simulated spectra of **2** in chloroform. Calculations were performed at the CAM-B3LYP/6-311++G(d,p) level of theory. Simulated spectra were shifted to match the experimental one.

Till now, we have discussed the results of simulations for systems where the experimental spectra exhibit a fine structure. It is a good test for the approach outlined in the present study to predict the absorption band shape without vibrational fine structure. For this reason we have considered a derivative of **1** with the (dimethylamino)phenyl substituent in the 4-position in DMF solution. Experimental data show that the absorption band corresponding to the bright $\pi \rightarrow \pi^*$ transition is structureless. To simulate this absorption band, we followed strictly the protocol used to simulate the spectra of molecule **2**, except that we performed rigid-body MD simulations for seven conformations. The interplanar angle was probed every 15° (from 0 to 90°), which resulted in 700 solute−solvent snapshots. The estimated standard deviation corresponding to a Gaussian distribution of vertical excitation energies was found to be 760 cm^{-1} (Γ_{INH} = 895 cm^{-1}). Likewise, in the wavepacket simulations, the lowest-frequency torsional mode was not included. The results of calculations are shown in Figure 6.

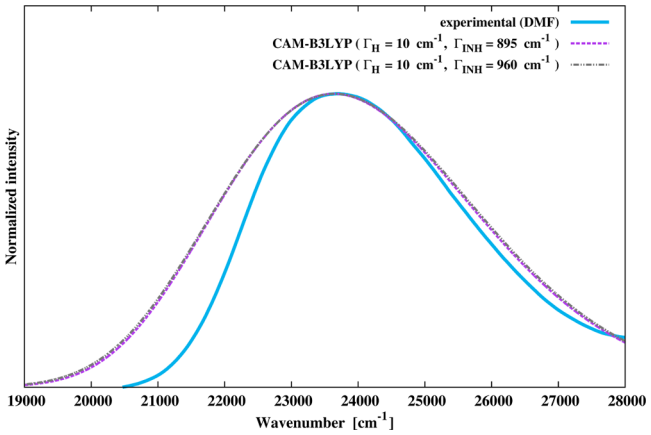

Figure 6. Experimental and simulated spectra of **3** in DMF. Calculations were performed at the CAM-B3LYP/6-311++G(d,p) level of theory. Simulated spectra were shifted to match the experimental one.

Even though the results of simulations show a slightly broader absorption band, it should not be overlooked that the simulations correctly predict smearing out the vibrational structure. Moreover, the choice of the value of inhomogeneous broadening has no significant influence on the spectral width of the band.

SUMMARY AND OUTLOOK

In this study we have presented the computational protocol suited for simulations of optical band shapes of molecules in solution. It involves several steps, including time-independent quantum-chemical calculations (electronic and vibrational structure), molecular dynamics simulations and time-dependent wavepacket simulations of vibrational fine structure of absorption bands. The advantage of the protocol presented herein is that it relies on the hybrid density functional theory/molecular mechanics approach, which retains the discrete representation of the solvent environment. It thus may be

dx.doi.org/10.1021/jp5094417 | J. Phys. Chem. A 2015, 119, 5145−5152

applied to estimate the inhomogeneous broadening for a large class of solute−solvent systems, including a scenario of specific interactions. As demonstrated in this study, the approach in question is a good choice for the modeling of spectra of rigid and semirigid chromophores. In the present study a focus was put on the bright $\pi \rightarrow \pi^*$ transition in three ketoimine difluoroborates and we employed the Condon approximation, thus neglecting coordinate dependence of the transition moment. It should not be overlooked, however, that the extension of the presented scheme to simulations of spectra at higher level of theory, i.e., including FC-HT and HT terms, is straightforward. Vibrational fine structure in multiphoton spectra can also be predicted in a like manner.

■ ASSOCIATED CONTENT

Supporting Information

Reaction schemes, synthetic details, NMR and FC spectra. This material is available free of charge via the Internet at http://pubs.acs.org.

■ AUTHOR INFORMATION

Corresponding Authors

*R. Zaleśny. E-mail: robert.zalesny@pwr.edu.pl.
*H. Ågren. E-mail: hagren@kth.se.

Notes

The authors declare no competing financial interest.

■ ACKNOWLEDGMENTS

The authors thank Dr. Anna Zakrzewska and Dr. Beata Jedrzejewska for their help in synthesis, purification, and measurements. R.Z. is a Wenner-Gren Foundations scholar. Financial support from the National Science Centre (Grant No. 2013/09/B/ST5/03550) is gratefully acknowledged. This research was supported in part by PL-Grid Infrastructure. The calculations were performed in part in the Wroclaw Center for Networking and Supercomputing. This work was also supported by the Swedish Infrastructure Committee (SNIC) for the project "Multiphysics Modeling of Molecular Materials", SNIC025/12-38.

■ REFERENCES

(1) Dreuw, A.; Head-Gordon, M. Single-Reference ab Initio Methods for the Calculation of Excited States of Large Molecules. *Chem. Rev.* **2005**, *105*, 4009.

(2) Casida, M. E. Time-Dependent Density-Functional Theory for Molecules and Molecular Solids. *J. Mol. Struct. (THEOCHEM)* **2009**, *914*, 3−18.

(3) Adamo, C.; Jacquemin, D. The Calculations of Excited-State Properties with Time-Dependent Density Functional Theory. *Chem. Soc. Rev.* **2013**, *42*, 845−856.

(4) Charaf-Eddin, A.; Planchat, A.; Mennucci, B.; Adamo, C.; Jacquemin, D. Choosing a Functional for Computing Absorption and Fluorescence Band Shapes with TD-DFT. *J. Chem. Theory Comput.* **2013**, *9*, 2749−2760.

(5) Laurent, A.; Jacquemin, D. TD-DFT Benchmarks: A Review. *Int. J. Quantum Chem.* **2013**, *113*, 2019−2039.

(6) Jacquemin, D.; Perpéte, E. A.; Scuseria, G. E.; Ciofini, I.; Adamo, C. TD-DFT Performance for the Visible Absorption Spectra of Organic Dyes: Conventional versus Long-Range Hybrids. *J. Chem. Theory Comput.* **2008**, *4*, 123−135.

(7) Jacquemin, D.; Wathelet, V.; Perpéte, E. A.; Adamo, C. Extensive TD-DFT Benchmark: Singlet-Excited States of Organic Molecules. *J. Chem. Theory Comput.* **2009**, *5*, 2420−2435.

(8) Jacquemin, D.; Moore, B.; Planchat, A.; Adamo, C.; Autschbach, J. Performance of an Optimally Tuned Range-Separated Hybrid Functional for 0−0 Electronic Excitation Energies. *J. Chem. Theory Comput.* **2014**, *10*, 1677−1685.

(9) Okuno, K.; Shigeta, Y.; Kishi, R.; Miyasaka, H.; Nakano, M. Tuned CAM-B3LYP Functional in the Time-Dependent Density Functional Theory Scheme for Excitation Energies and Properties of Diarylethene Derivatives. *J. Photochem. Photobiol., A* **2012**, *235*, 29−34.

(10) Vivas, M. G.; Silva, D. L.; Malinge, J.; Boujtita, M.; Zaleśny, R.; Bartkowiak, W.; Ågren, H.; Canuto, S.; Boni, L. D.; Ishow, E.; et al. Molecular Structure - Optical Property Relationships for a Series of Non-Centrosymmetric Two-photon Absorbing Push-Pull Triarylamine Molecules. *Sci. Rep.* **2014**, *4*, 4447.

(11) Bednarska, J.; Roztoczyńska, A.; Bartkowiak, W.; Zaleśny, R. Comparative Assessment of Density Functionals for Excited-State Dipole Moments. *Chem. Phys. Lett.* **2013**, *584*, 58−62.

(12) Lasorne, B.; Jornet-Somoza, J.; Meyer, H.-D.; Lauvergnat, D.; Robb, M. A.; Gatti, F. Vertical Transition Energies vs. Absorption Maxima: Illustration with the UV Absorption Spectrum of Ethylene. *Spectrochim. Acta, Part A* **2014**, *119*, 52−58.

(13) Baiardi, A.; Bloino, J.; Barone, V. General Time Dependent Approach to Vibronic Spectroscopy Including Franck-Condon, Herzberg-Teller, and Duschinsky Effects. *J. Chem. Theory Comput.* **2013**, *9*, 4097−4115.

(14) Silverstein, D. W.; Jensen, L. Vibronic Coupling Simulations for Linear and Nonlinear Optical Processes: Simulation Results. *J. Chem. Phys.* **2012**, *136*, 064110.

(15) Weiss, P. A.; Silverstein, D. W.; Jensen, L. Non-Condon Effects on the Doubly Resonant Sum Frequency Generation of Rhodamine 6G. *J. Phys. Chem. Lett.* **2014**, *5*, 329−335.

(16) Petrenko, T.; Neese, F. Efficient and Automatic Calculation of Optical Band Shapes and Resonance Raman Spectra for Larger Molecules Within the Independent Mode Displaced Harmonic Oscillator Model. *J. Chem. Phys.* **2012**, *137*, 234107.

(17) Silverstein, D. W.; Govind, N.; van Dam, H. J. J.; Jensen, L. Simulating One-Photon Absorption and Resonance Raman Scattering Spectra Using Analytical Excited State Energy Gradients within Time-Dependent Density Functional Theory. *J. Chem. Theory Comput.* **2013**, *9*, 5490−5503.

(18) Heller, E. J. The Semiclassical Way to Molecular Spectroscopy. *Acc. Chem. Res.* **1981**, *14*, 368−375.

(19) Silverstein, D. W.; Jensen, L. Vibronic Coupling Simulations for Linear and Nonlinear Optical Processes: Theory. *J. Chem. Phys.* **2012**, *136*, 064111.

(20) Chibani, S.; Charaf-Eddin, A.; Mennucci, B.; Le Guennic, B.; Jacquemin, D. Optical Signatures of OBO Fluorophores: A Theoretical Analysis. *J. Chem. Theory Comput.* **2014**, *10*, 805−815.

(21) Charaf-Eddin, A.; Le Guennic, B.; Jacquemin, D. Optical Signatures of Borico Dyes: a TD-DFT analysis. *Theor. Chem. Acc.* **2014**, *133*, 1456.

(22) Houari, Y.; Laurent, A. D.; Jacquemin, D. Spectral Signatures of Perylene Diimide Derivatives: Insights From Theory. *J. Phys. Chem. C* **2013**, *117*, 21682−21691.

(23) Zakrzewska, A.; Zaleśny, R.; Kolehmainen, E.; Ośmiałowski, B.; Jedrzejewska, B.; Ågren, H.; Pietrzak, M. Substituent Effects on the Photophysical Properties of Fluorescent 2-benzoylmethylenequinoline Difluoroboranes: A Combined Experimental and Quantum Chemical Study. *Dyes Pigm.* **2013**, *99*, 957−965.

(24) Chibani, S.; Charaf-Eddin, A.; Le Guennic, B.; Jacquemin, D. Boranil and Related NBO Dyes: Insights From Theory. *J. Chem. Theory Comput.* **2013**, *9*, 3127−3135.

(25) Le Guennic, B.; Chibani, S.; Charaf-Eddin, A.; Massue, J.; Ziessel, R.; Ulrich, G.; Jacquemin, D. The NBO Pattern in Luminescent Chromophores: Unravelling Excited-State Features Using TD-DFT. *Phys. Chem. Chem. Phys.* **2013**, *15*, 7534−7540.

(26) Chibani, S.; Le Guennic, B.; Charaf-Eddin, A.; Maury, O.; Andraud, C.; Jacquemin, D. On the Computation of Adiabatic Energies in Aza-Boron-Dipyrromethene Dyes. *J. Chem. Theory Comput.* **2012**, *8*, 3303−3313.

(27) Jacquemin, D.; Planchat, A.; Adamo, C.; Mennucci, B. TD-DFT Assessment of Functionals for Optical 0−0 Transitions in Solvated Dyes. *J. Chem. Theory Comput.* **2012**, *8*, 2359−2372.
(28) Jacquemin, D.; Bremond, E.; Ciofini, I.; Adamo, C. Impact of Vibronic Couplings on Perceived Colors: Two Anthraquinones as a Working Example. *J. Phys. Chem. Lett.* **2012**, *3*, 468−471.
(29) Jacquemin, D.; Bremond, E.; Planchat, A.; Ciofini, I.; Adamo, C. TD-DFT Vibronic Couplings in Anthraquinones: From Basis Set and Functional Benchmarks to Applications for Industrial Dyes. *J. Chem. Theory Comput.* **2011**, *7*, 1882−1892.
(30) De Mitri, N.; Monti, S.; Prampolini, G.; Barone, V. Absorption and Emission Spectra of a Flexible Dye in Solution: A Computational Time-Dependent Approach. *J. Chem. Theory Comput.* **2013**, *9*, 4507−4516.
(31) Mercer, I. P.; Gould, I. R.; Klug, D. R. Optical Properties of Solvated Molecules Calculated by a QMMM Method Chlorophyll *a* and Bacteriochlorophyll *a*. *Faraday Discuss.* **1997**, *108*, 51−62.
(32) Walker, R. C.; de Souza, M. M.; Mercer, I. P.; Gould, I. R.; King, D. R. Large and Fast Relaxations Inside a Protein: Calculation and Measurement of Reorganization Energies in Alcohol Dehydrogenase. *J. Phys. Chem. B* **2002**, *106*, 11658−11665.
(33) Mercer, I. P.; Gould, I. R.; King, D. R. A Quantum Mechanical/Molecular Mechanical Approach to Relaxation Dynamics: Calculation of the Optical Properties of Solvated Bacteriochlorophyll-a. *J. Phys. Chem. B* **1999**, *103*, 7720−7727.
(34) Isborn, C. M.; Götz, A. W.; Clark, M. A.; Walker, R. C.; Martínez, T. J. Electronic Absorption Spectra from MM and ab Initio QM/MM Molecular Dynamics: Environmental Effects on the Absorption Spectrum of Photoactive Yellow Protein. *J. Phys. Chem. B* **2012**, *8*, 5092−5106.
(35) Murugan, N. A.; Zaleśny, R.; Kongsted, J.; Ågren, H. Chelation-Induced Quenching of Two-Photon Absorption of Azacrown Ether Substituted Distyryl Benzene for Metal Ion Sensing. *J. Chem. Theory Comput.* **2014**, *10*, 778−788.
(36) Fonseca, T. L.; Coutinho, K.; Canuto, S. Polarization and Solvatochromic Shift of *ortho*-betaine in Water. *Chem. Phys.* **2008**, *349*, 109−114.
(37) Silva, D. L.; Murugan, N. A.; Kongsted, J.; Rinkevicius, Z.; Canuto, S.; Ågren, H. The Role of Molecular Conformation and Polarizable Embedding for One- and Two-Photon Absorption of Disperse Orange 3 in Solution. *J. Phys. Chem. B* **2012**, *116*, 8169−8181.
(38) Eilmes, A. Effect of Molecular Vibrations on the MD/QC-Simulated Absorption Spectra. *Int. J. Quantum Chem.* **2014**, *114*, 261−270.
(39) Tomasi, J.; Persico, M. Molecular Interactions in Solution: An Overview of Methods Based on Continuous Distributions of the Solvent. *Chem. Rev.* **1994**, *94*, 2027−2094.
(40) Tomasi, J.; Mennucci, B.; Cammi, R. Quantum Mechanical Continuum Solvation Models. *Chem. Rev.* **2005**, *105*, 2999−3094.
(41) Ai, Y.; Tian, G.; Luo, Y. Role of Non-Condon Vibronic Coupling and Conformation Change on Two-Photon Absorption Spectra of Green Fluorescent Protein. *Mol. Phys.* **2013**, *111*, 1316−1321.
(42) Ferrer, F. J. A.; Improta, R.; Santoro, F.; Barone, V. Computing the Inhomogeneous Broadening of Electronic Transitions in Solution: a First-Principle Quantum Mechanical Approach. *Phys. Chem. Chem. Phys.* **2011**, *13*, 17007−17012.
(43) Ferrer, F. J. A.; Cerezo, J.; Soto, J.; Improta, R.; Santoro, F. First-Principle Computation of Absorption and Fluorescence Spectra in Solution Accounting for Vibronic Structure, Temperature Effects and Solvent Inhomogenous Broadening. *Comput. Theor. Chem.* **2014**, *1040−1041*, 328−337.
(44) Yanai, T.; Tew, D. P.; Handy, N. C. A New Hybrid Exchange-Correlation Functional Using the Coulomb-Attenuating Method (CAM-B3LYP). *Chem. Phys. Lett.* **2004**, *393*, 51−57.
(45) Guido, C. A.; Knecht, S.; Kongsted, J.; Mennucci, B. Benchmarking Time-Dependent Density Functional Theory for Excited State Geometries of Organic Molecules in Gas-Phase and in Solution. *J. Chem. Theory Comput.* **2013**, *9*, 2209−2220.
(46) Cammi, R.; Mennucci, B. Linear Response Theory for the Polarizable Continuum Model. *J. Chem. Phys.* **1999**, *110*, 9877−9886.
(47) Cossi, M.; Barone, V. Time-Dependent Density Functional Theory for Molecules in Liquid Solutions. *J. Chem. Phys.* **2001**, *115*, 4708−4717.
(48) Frisch, M. J.; et al. *GAUSSIAN 09*, Revision D.01; Gaussian Inc.: Wallingford, CT, 2009.
(49) Hättig, C.; Weigend, F. CC2 Excitation Energy Calculations on Large Molecules Using the Resolution of the Identity Approximation. *J. Chem. Phys.* **2000**, *113*, 5154−5161.
(50) *TURBOMOLE* V6.4 2012, a Development of University of Karlsruhe and Forschungszentrum Karlsruhe GmbH, 1989−2007, TURBOMOLE GmbH, since 2007; available from http://www.turbomole.com.
(51) Amirjalayer, S.; Snurr, R. Q.; Schmid, R. Prediction of Structure and Properties of Boron-Based Covalent Organic Frameworks by a First-Principles Derived Force Field. *J. Phys. Chem. C* **2012**, *116*, 4921−4929.
(52) Wang, J.; Wolf, R. M.; Caldwell, J. W.; Kollman, P. A.; Case, D. A. Development and Testing of a General AMBER Force Field. *J. Comput. Chem.* **2004**, *25*, 1157−1174.
(53) Breneman, C. M.; Wiberg, K. B. Determining Atom-Centered Monopoles from Molecular Electrostatic Potentials. The Need for High Sampling Density in Formamide Conformational Analysis. *J. Comput. Chem.* **1990**, *11*, 361−373.
(54) Case, D. A.; et al. *AMBER 11*; University of California: San Francisco, 2010.
(55) Nielsen, C. B.; Christiansen, O.; Mikkelsen, K. V.; Kongsted, J. Density Functional Self-Consistent Quantum Mechanics/Molecular Mechanics Theory for Linear and Nonlinear Molecular Properties: Applications to Solvated Water and Formaldehyde. *J. Chem. Phys.* **2007**, *126*, 154112.
(56) Schwabe, T.; Sneskov, K.; Haugaard Olsen, J. M.; Kongsted, J.; Christiansen, O.; Hattig, C. PERI-CC2: A Polarizable Embedded RI-CC2Method. *J. Chem. Theory Comput.* **2012**, *8*, 3274−3283.
(57) Gagliardi, L.; Lindh, R.; Karlström, G. Local Properties of Quantum Chemical Systems: The LoProp Approach. *J. Chem. Phys.* **2004**, *121*, 4494−4500.
(58) Aidas, K.; et al. The Dalton Quantum Chemistry Program System. *Wiley Interdiscip. Rev.: Comput. Mol. Sci.* **2014**, *4*, 269−284.
(59) Petrenko, T.; Neese, F. Analysis and Prediction of Absorption Band Shapes, Fluorescence Band Shapes, Resonance Raman Intensities, and Excitation Profiles Using the Time-Dependent Theory of Electronic Spectroscopy. *J. Chem. Phys.* **2007**, *127*, 164319.
(60) Neese, F. The ORCA program system. *Wiley Interdiscip. Rev.: Comput. Mol. Sci.* **2012**, *2*, 73−78.
(61) Frath, D.; Massue, J.; Ulrich, G.; Ziessel, R. Luminescent Materials: Locking π-Conjugated and Heterocyclic Ligands with Boron(III). *Angew. Chem., Int. Ed.* **2014**, *53*, 2290−2310.
(62) Gotor, R.; Costero, A. M.; Gil, S.; Gavina, P.; Rurack, K. On the Ion-Pair Recognition and Indication Features of a Fluorescent Heteroditopic Host Based on a BODIPY Core. *Eur. J. Org. Chem.* **2014**, 4005−4013.
(63) Singh, S. P.; Gayathri, T. Evolution of BODIPY Dyes as Potential Sensitizers for Dye-Sensitized Solar Cells. *Eur. J. Org. Chem.* **2014**, 4689−4707.
(64) Ni, Y.; Wu, J. Far-red and Near Infrared BODIPY Dyes: Synthesis and Applications for Fluorescent pH Probes and Bio-Imaging. *Org. Biomol. Chem.* **2014**, *12*, 3774−3791.
(65) Pan, Z.-H.; Luo, G.-G.; Zhou, J.-W.; Xia, J.-X.; Fang, K.; Wu, R.-B. A Simple BODIPY-aniline-based Fluorescent Chemosensor as Multiple Logic Operations for the Detection of pH and CO_2 Gas. *Dalton Trans.* **2014**, *43*, 8499−8507.
(66) Yu, X.; Jia, X.; Yang, X.; Liu, W.; Qin, W. Synthesis and Photochemical Properties of BODIPY-Functionalized Silica Nanoparticle for Imaging Cu^{2+} in Living cells. *RSC Adv.* **2014**, *4*, 23571−23579.

(67) Myers, A. B. Molecular Electronic Spectral Broadening In Liquids and Glasses. *Annu. Rev. Phys. Chem.* **1998**, *49*, 267−95.
(68) Boulanger, P.; Chibani, S.; Guennic, B. L.; Duchemin, I.; Blase, X.; Jacquemin, D. Combining the Bethe-Salpeter Formalism with Time-Dependent DFT Excited-State Forces to Describe Optical Signatures: NBO Fluoroborates as Working Examples. *J. Chem. Theory Comput.* **2014**, *10*, 4548−4556.